PERGAMON

International Journal of Solids and Structures 37 (2000) 6555–6570

INTERNATIONAL JOURNAL OF SOLIDS and STRUCTURES

www.elsevier.com/locate/ijsolstr

Stress intensity factor and effective stiffness of a solid containing aligned penny-shaped cracks

V.I. Kushch [a,*], A.S. Sangani [b]

[a] *Institute for Superhard Materials, National Academy of Sciences, 254074 Kiev, Ukraine*
[b] *Department of Chemical Engineering and Material Science, Syracuse University, Syracuse, NY 13244, USA*

Received 12 April 1999; in revised form 11 October 1999

Abstract

The stress state and effective elastic moduli of an isotropic solid containing equally oriented penny-shaped cracks are evaluated accurately. The geometric model of a cracked body is a spatially periodic medium whose unit cell contains a number of arbitrarily placed aligned circular cracks. A rigorous analytical solution of the boundary-value problem of the elasticity theory has been obtained using the technique of triply periodic solutions of the Lame equation. By exact satisfaction of the boundary conditions on the cracks' surfaces, the primary problem is reduced to solving an infinite set of linear algebraic equations. An asymptotic analysis of the stress field has been performed and the exact formulae for the stress intensity factor (SIF) and effective elasticity tensor are obtained. The numerical results are presented demonstrating the effect of the crack density parameter and arrangement type on SIF and overall elastic response of a solid and comparison is made with known approximate theories.

Keywords: Elasticity; Crack; Stiffness; Stress intensity factor; Multipole expansion

1. Introduction

The cracks are probably the most common structural defects in solid materials. Their presence could significantly influence the stiffness and brittle strength of a solid. Thus, for example, the elastic moduli of the solid decrease with the increasing crack density, and the oriented cracks render the overall material anisotropic. The cracks also induce significant local stress concentrations and thereby increase the risk of rupture. The stress intensity factor (SIF) at the crack's tip is often used to predict the failure load and, therefore, has the theoretical as well as practical

* Corresponding author.
E-mail address: vkushch@ecs.syr.edu (V.I. Kushch).

0020-7683/00/$ - see front matter
PII: S0020-7683(99)00288-7

interest. Both the elastic moduli and SIF are strongly dependent on the density and the geometrical arrangement of cracks. Hence, for a reliable prediction of elastic behavior of a cracked solid, it is necessary: (1) to use a geometrical model that reflects the structure of actual material and (2) to account for the crack interactions accurately.

The problem of predicting the overall elastic properties of cracked solids has been examined by a number of investigators. Practically, all the approaches developed for predicting the elastic properties of composite materials have also been applied to the materials with cracks. An elliptic crack can be thought of as an ellipsoidal cavity with one of its axes tending to zero. In other words, a "penny-shaped" crack used by most investigators to model the cracks in a (three-dimensional) solid is nothing but an infinitely thin oblate spheroidal cavity. Thus, in principle, all the results known for composites with ellipsoidal inclusions may be extended to cracked materials by proper limiting process. The variational bounds for the effective moduli of a cracked material were established by Willis (1980). Among the methods accounting for the crack interactions in an approximate way, we mention the self-consistent scheme (Budiansky and O'Connell, 1976; Hoenig, 1979; Laws and Brockenbrough, 1987), the Mori–Tanaka's method (Benveniste, 1986), and the differential scheme (Salganik, 1973; Heyney and Pomphrey, 1982; Laws and Dvorak, 1987; Hashin, 1988). All these methods are based on so-called "one-particle" model, being a single crack embedded in an "effective" homogeneous medium. None of them define explicitly (and, hence, take into account) the actual microstructure of a cracked solid: the only structure parameter used is the number density of cracks.

One possible way to account for the crack orientation statistics was developed by Kachanov (1987, 1993), who introduced the crack density tensor and used the tensorial linearization of the elastic potential to obtain a simple estimate for the effective elastic moduli. An alternate approach, known in the composite mechanics as the "regularization" method (e.g., Golovchan et al., 1993), is based on modeling the structure of actual non-homogeneous solid by a periodic medium whose unit cell contains a number of inclusions. This approach appears to be promising in that the detailed geometric arrangement of the inclusions can be specified explicitly. Moreover, due to deterministic nature of the given model, it is possible to state and solve accurately the periodic boundary-value problems of interest and to thereby account for the interactions among the inclusions in a rigorous manner. Recently, this approach was combined successfully with the multipole expansion technique to study the elastic behavior of the composites reinforced by the spherical (Sangani and Mo, 1997) and spheroidal (Kushch, 1998) particles. As to the cracked materials, only the simplest periodic structures were considered before. For a solid containing a simple orthogonal array of penny-shaped cracks, an approximate solution was obtained by Nemat-Nasser et al. (1993), who used the Fourier series technique and assumed the homogenization eigenstrains to be uniform. The same structure was also analyzed by Fares (1993), who used the boundary element method to take into account interactions of a finite number of cracks. Thus, to the best of our knowledge, only approximate solutions are available at present in the mechanics of 3D solids with cracks.

In the present paper, an accurate series method will be developed based on the generalized periodic structure model of a cracked solid. Section 2 describes the model and the governing equations. Section 3 outlines the method of solution, which is a direct extension of the method proposed by Kushch (1997) to study elastic behavior of a heterogeneous solid with spheroidal interfaces. The exact expressions for the effective moduli are derived by averaging the stress and strain tensors. Also given is a series expansion for the SIF obtained by an asymptotic analysis of the stress field singularity at the crack's tip. Finally, in Section 4, the results of numerical simulations for the solids with various arrangements of cracks are presented and compared with known approximate theories.

2. Statement of the problem

Let us consider an isotropic medium containing a spatially periodic array of equally oriented penny-shaped cracks. Its elementary unit cell in the form of parallelepiped with the sides a_1, a_2 and a_3 containing the centers of N cracks is shown in Fig. 1. The volume of this unit cell is $V = a_1a_2a_3$. The global Cartesian coordinate system $Oxyz$ is introduced so that the crack's surfaces are parallel to the Oxy plane. Also, we define the local Cartesian coordinate systems $O_px_py_pz_p$, $p = \overline{1, N}$. The origin of pth coordinate system O_p coincides with the center of pth crack of radius d_p, the axes O_px_p, O_py_p and O_pz_p are parallel to the global axes Ox, Oy and Oz, respectively. The vector $\mathbf{R}_p=(X_p, Y_p, Z_p)$ determines the position of pth crack. Also, $\mathbf{r}_p=(x_p, y_p, z_p)$ is the local radius vector and $\mathbf{r} = (x, y, z)$ is the global one: $\mathbf{r}_p = \mathbf{r}_q + \mathbf{R}_{pq}$ and $\mathbf{r} = \mathbf{r}_p + \mathbf{R}_p$, where $\mathbf{R}_{pq} = \mathbf{R}_p - \mathbf{R}_q$. The placement of the rest of the cracks is determined by adding to $\mathbf{R}_p$ the translation vector $\mathbf{V}_n=n_1a_1\mathbf{e}_x+n_2a_2\mathbf{e}_y+n_3a_3\mathbf{e}_z$, where n_i are the integers, $-\infty < n_1, n_2, n_3 < \infty$.

Now, we introduce the oblate spheroidal coordinates $(f_p, \xi_p, \eta_p, \varphi_p)$, related to the Cartesian ones by (Hobson, 1931)

$$x_p + iy_p = f_p\xi_p\bar{\eta}_p \exp(i\varphi_p), \quad z_p = f_p\bar{\xi}_p\eta_p;$$

$$\bar{\xi}_p^2 = \xi_p^2 - 1, \quad \bar{\eta}_p^2 = 1 - \eta_p^2; \qquad 1 \le \xi_p < \infty, |\eta_p| \le 1, 0 \le \varphi_p < 2\pi. \tag{1}$$

The equation (1) for $\xi_p = \text{const}$ describes a family of confocal oblate spheroids. In particular, the value $\xi_p = 1$ corresponds to the surface of pth crack coinciding with the focal disc of pth local spheroidal coordinate system. It was shown elsewhere (Kushch, 1998) that the spheroidal coordinates is quite natural and useful to treat the crack problems because they provide an efficient way to satisfy the boundary conditions of the crack's surface.

We suppose that the stress state of a cracked medium is induced by the remote constant strain tensor $\hat{\mathbf{E}} = E_{ij}$. The displacement vector $\mathbf{u}$ in a solid phase satisfies the Lame equation

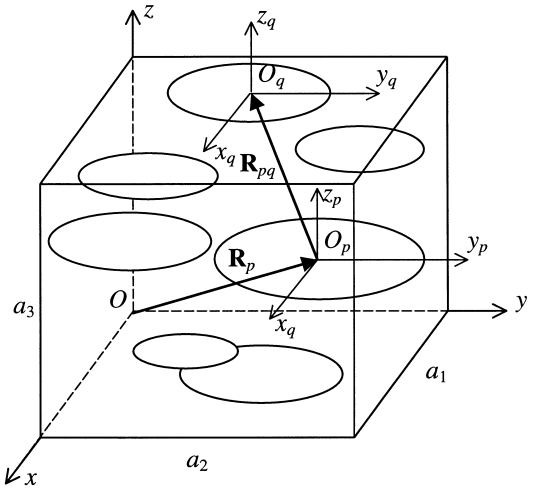

Fig. 1. Unit cell of a generalized periodic structure model of cracked solid.

$$2(1-\nu)\nabla(\nabla\cdot\mathbf{u})-(1-2\nu)\nabla\times\nabla\times\mathbf{u}=\mathbf{0} \tag{2}$$

where ν is the Poisson's ratio. The crack's surfaces are assumed to be load-free:

$$\mathbf{T}_{\xi}(\mathbf{u})\big|_{\xi_q=1}=0,\quad q=1,2,\ldots,N; \tag{3}$$

where $\mathbf{T}_{\xi}=\sigma_{\xi}\mathbf{e}_{\xi}+\tau_{\xi\eta}\mathbf{e}_{\eta}+\tau_{\xi\varphi}\mathbf{e}_{\varphi}$ is a surface traction vector. In the limiting case $\xi_p=1$ ($\bar{\xi}_p=0$), we have

$$\mathbf{T}_{\xi}=\mathbf{T}_z=\tau_{xz}\mathbf{e}_x+\tau_{yz}\mathbf{e}_y+\sigma_z\mathbf{e}_z. \tag{4}$$

Due to periodicity of the structure and the uniformity of the external loading, the resulting strain and stress fields are macroscopically uniform and, hence, periodic functions of spatial coordinates. In this case, the displacement vector $\mathbf{u}$ can be represented as a sum of the linear and periodic terms:

$$\mathbf{u}=\hat{\mathbf{E}}\cdot\mathbf{r}+\mathbf{u}_1, \tag{5}$$

where

$$\mathbf{u}_1(\mathbf{r})=\mathbf{u}_1(\mathbf{r}-a_1\mathbf{e}_x)=\mathbf{u}_1(\mathbf{r}-a_2\mathbf{e}_y)=\mathbf{u}_1(\mathbf{r}-a_3\mathbf{e}_z) \tag{6}$$

and $\hat{\mathbf{E}}$ has a sense of macroscopic strain tensor, i.e.

$$E_{ij}=\bar{\varepsilon}_{ij}=\frac{1}{2V}\int_{S_e}(u_in_j+u_jn_i)\,\mathrm{d}S. \tag{7}$$

Here, S_e is the external boundary of unit cell and n_i are the Cartesian components of outward unit normal vector at the cell boundary. We will suppose $\hat{\mathbf{E}}$ to be given: thus, the problem is to construct the periodic vectorial function $\mathbf{u}_1$ in such a way so as to satisfy the equilibrium equation (2) and boundary conditions (3).

3. Method of solution

The basic method is described in detail elsewhere (Kushch, 1996, 1997). Here, we briefly outline the important steps. We write $\mathbf{u}_1$ as a series

$$\mathbf{u}_1(\mathbf{r})=\sum_{p=1}^{N}\mathbf{U}^{(p)},\quad \mathbf{U}^{(p)}=\sum_{i=1}^{3}\sum_{t=1}^{\infty}\sum_{s=-t}^{t}A_{ts}^{(i)(p)}\mathbf{S}_{ts}^{*(i)}(\mathbf{r}_p,f_p), \tag{8}$$

where $A_{ts}^{(i)(p)}$ are arbitrary constants. The vectorial functions

$$\mathbf{S}_{ts}^{*(i)}(\mathbf{r},f)=\sum_{\mathrm{n}}\mathbf{S}_{ts}^{(i)}(\mathbf{r}+\mathbf{V}_{\mathrm{n}},f) \tag{9}$$

are triply periodic singular solutions of the Lame equation (Kushch, 1997) and $\mathbf{S}_{ts}^{(i)}$ are the singular vectorial solutions of Eq. (2) given by formula (A1) of Appendix A, where in the case of penny-shaped cracks, one should put $\xi_p^{(0)}=0$.

The displacement vector in the form (8) and (9) satisfies the differential equation (2) and the periodicity conditions (6). To satisfy the boundary conditions (3) for, say, the qth crack, we need to have a local expansion of $\mathbf{u}$ in the qth spheroidal coordinate system. Such an expansion of the linear part of Eq. (5) has a form

$$\hat{\mathbf{E}}\cdot\mathbf{r}=\sum_{i=1}^{3}\sum_{t=0}^{\infty}\sum_{s=-t}^{t}e_{ts}^{(i)(q)}\mathbf{s}_{ts}^{(i)}(\mathbf{r}_q,f_q), \tag{10}$$

where $\mathbf{s}_{ts}^{(i)(q)}$ are the regular partial solutions of the Lame equation (A2) and

$$e_{10}^{(1)(q)}=E_{13}X_q+E_{23}Y_q+E_{33}Z_q;$$

$$e_{11}^{(1)(q)}=-\overline{e_{1,-1}^{(1)(q)}}=(E_{11}-iE_{12})X_q+(E_{21}-iE_{22})Y_q+(E_{31}-iE_{32})Z_q;$$

$$e_{00}^{(3)(q)}=\frac{f_q}{2(2\nu-1)}(E_{11}+E_{22}+E_{33});$$

$$e_{20}^{(1)(q)}=\frac{f_q}{3}(2E_{33}-E_{11}-E_{22});$$

$$e_{21}^{(1)(q)}=-\overline{e_{2,-1}^{(1)(q)}}=f_q(E_{13}-iE_{23});$$

$$e_{22}^{(1)(q)}=\overline{e_{2,-2}^{(1)(q)}}=f_q(E_{11}-iE_{22}-2E_{12}); \tag{11}$$

all other $e_{ts}^{(i)(q)}$ are equal to zero.

The series expansion of the periodic part of $\mathbf{u}$, obtained from Eq. (8) with the aid of addition theorems for the singular partial solutions (Kushch, 1996)

$$\mathbf{S}_{ts}^{(i)}(\mathbf{r}_p,f_p)=\sum_{j=1}^{3}\sum_{k=0}^{\infty}\sum_{l=-k}^{k}\eta_{tksl}^{(i)(j)}(\mathbf{R}_{pq},f_p,f_q)\mathbf{s}_{kl}^{(j)}(\mathbf{r}_q,f_q),\quad i=1,2,3;\ t=1,2,\ldots;\ |s|\le t; \tag{12}$$

has a form

$$\mathbf{u}_1(\mathbf{r}_q)=\sum_{i=1}^{3}\sum_{t=1}^{\infty}\sum_{s=-t}^{t}A_{ts}^{(i)(q)}\mathbf{S}_{ts}^{(i)}(\mathbf{r}_q,f_q)+\sum_{i=1}^{3}\sum_{t=0}^{\infty}\sum_{s=-t}^{t}e_{ts}^{(i)(q)}\mathbf{s}_{ts}^{(i)}(\mathbf{r}_q,f_q), \tag{13}$$

where

$$a_{ts}^{(i)(q)}=\sum_{p=1}^{N}\sum_{j=1}^{3}\sum_{k=0}^{\infty}\sum_{l=-k}^{k}\eta_{ktls}^{*(j)(i)}(\mathbf{R}_{pq},f_p,f_q)A_{kl}^{(j)(p)}$$

and

$$\eta_{tksl}^{*(i)(j)}(\mathbf{R}_{pq},f_p,f_q)=\sum_{\mathrm{n}}\eta_{tksl}^{(i)(j)}(\mathbf{R}_{pq}+\mathbf{V}_{\mathrm{n}},f_p,f_q). \tag{14}$$

The explicit form of the expansion coefficients $\eta_{tksl}^{(i)(j)}$ as well as the efficient technique for calculating the sums (14) are given in Kushch (1997). Substituting the expansions (10) and (13) into Eq. (5) and then into Eq. (3), one obtains, after, some algebra, an infinite set of linear algebraic equations in unknowns $A_{ts}^{(i)(p)}$ which can be written in the matrix form as

$$TG_t^{(q)}(\nu)\mathbf{A}_t^{(q)} + TM_t^{(q)}(\nu)\mathbf{a}_t^{(q)} = -TM_t^{(q)}(\nu)\mathbf{e}_t^{(q)}, \quad q = 1, 2, \ldots, N;\ t = 1, 2, \ldots \tag{15}$$

Here, the vector $\mathbf{A}_t^{(q)}$ contains unknowns $A_{t+i-2,\,s}^{(i)(q)}$ and the vectors $\mathbf{a}_t^{(q)}$ and $\mathbf{e}_t^{(q)}$ are composed from the values $a_{t-i+2,\,s}^{(i)(q)}$ and $e_{t-i+2,\,s}^{(i)(q)}$, respectively; the matrices TG_t and TM_t are defined in Kushch (1996). The infinite set (15) has the normal type determinant and, therefore, its solution can be found with any desirable accuracy by solving the truncated system (15) with $t \le t_{\max}$.

Now, we find the effective, or macroscopic, stiffness tensor $\hat{\mathbf{C}} = \{C_{ijkl}\}$ of a cracked solid defined by the relation

$$\bar{\sigma}_{ij} = C_{ijkl}\bar{\varepsilon}_{kl}, \quad \bar{\sigma}_{ij} = \frac{1}{V}\int_V \sigma_{ij}\,\mathrm{d}V. \tag{16}$$

All we need to determine $\hat{\mathbf{C}}$ is to derive the expressions for $\bar{\sigma}_{ij}$ and calculate them for selected values of $\bar{\varepsilon}_{kl} = E_{kl}$.

The integration procedure used here is somewhat different from that applied by Kushch (1997) and does not imply integration over the inclusion volume. Because in the solid phase $\sigma_{ij} = C_{ijkl}^{(0)}\varepsilon_{kl} = 2\mu(\varepsilon_{ij} + \delta_{ij}\frac{\nu}{1-2\nu}\varepsilon_{kk})$, one obtains easily with the aid of Gauss' theorem

$$\bar{\sigma}_{ij} = \frac{1}{V}\int_V \sigma_{ij}\,\mathrm{d}V = C_{ijkl}^{(0)}\frac{1}{V}\int_V \varepsilon_{kl}\,\mathrm{d}V = C_{ijkl}^{(0)}\left[\bar{\varepsilon}_{kl} + \frac{1}{2V}\sum_{p=1}^{N}\int_{S_p}(u_k n_l + u_l n_k)\,\mathrm{d}S\right],$$

where S_p is the surface of pth crack. Calculation of the surface integrals uses the expansions (10) and (13) and gives us

$$\frac{\bar{\sigma}_{11} + \bar{\sigma}_{22} + \bar{\sigma}_{33}}{3K} = E_{11} + E_{22} + E_{33} - \left(1 + \frac{4\mu}{3K}\right)\sum_{p=1}^{N}\tilde{f}_p A_{00}^{(1)(p)}; \tag{17}$$

$$\frac{2\bar{\sigma}_{33} - \bar{\sigma}_{11} - \bar{\sigma}_{22}}{2\mu} = 2E_{33} - E_{11} - E_{22} + 4(1-\nu)\sum_{p=1}^{N}\tilde{f}_p A_{20}^{(3)(p)};$$

$$\frac{\bar{\sigma}_{11} - \bar{\sigma}_{22} - 2i\bar{\sigma}_{12}}{2} = E_{11} - E_{22} - 2iE_{12} + 8(1-\nu)\sum_{p=1}^{N}\tilde{f}_p A_{22}^{(3)(p)};$$

$$\frac{\bar{\sigma}_{13} - i\bar{\sigma}_{23}}{2\mu} = E_{13} - iE_{23} + 4(1-\nu)\sum_{p=1}^{N}\tilde{f}_p A_{21}^{(3)(p)};$$

where $\tilde{f}_p = 4\pi(f_p)^2/3V$ and $K = [2\mu(1+\nu)]/[3(1-2\nu)]$ is the bulk modulus of the matrix material. The expressions (17) are exact and contain only the first few unknowns $A_{ts}^{(i)(p)}$ which can be found from the truncated system (15) at moderate values of index $t = t_{\max}$ retained.

Note that to solve the problems (2) and (3) with the macroscopic stresses $\bar{\sigma}_{ij}$ prescribed as the external loading parameters, it is sufficient to invert the relations (17) and substitute the expressions of E_{ij} obtained in the right-side vector of Eq. (15). This type of problem statement is natural and convenient, in particular, when the stress concentration in composite or SIF in a cracked material is considered. The last ones are defined by the relations (e.g., Budiansky and O'Connell, 1976)

Table 1
Convergence test of E^*_{33}, μ^*_{13} and $\langle K^*_{\mathrm{I}}\rangle$ with increasing $t_{\max}$

$t_{\max}$	$a_1 = 2.2$			$a_1 = 2.01$		
	E^*_{33}/E	μ^*_{13}/μ	$\langle K^*_{\mathrm{I}}\rangle/K_{\mathrm{I}\infty}$	E^*_{33}/E	μ^*_{13}/μ	$\langle K^*_{\mathrm{I}}\rangle/K_{\mathrm{I}\infty}$
1	0.4544	0.4511	0.639	0.3396	0.3412	0.790
3	0.4306	0.4401	1.029	0.3075	0.3249	1.364
5	0.4302	0.4401	1.101	0.3063	0.3231	1.515
7	0.4301	0.4400	1.087	0.3062	0.3228	1.528
9	0.4301	0.4400	1.082	0.3061	0.3226	1.539
11	0.4301	0.4400	1.083	0.3061	0.3226	1.551
13	0.4301	0.4400	1.083	0.3060	0.3225	1.559
15	0.4301	0.4400	1.083	0.3060	0.3225	1.561

$$K_{\mathrm{I}} = \lim_{r\to 0}\sqrt{2\pi r}\sigma_z\Big|_{z=0};\quad K_{\mathrm{II}} = \lim_{r\to 0}\sqrt{2\pi r}\tau_{rz}\Big|_{z=0};\quad K_{\mathrm{III}} = \lim_{r\to 0}\sqrt{2\pi r}\tau_{z\varphi}\Big|_{z=0};$$

where r is the distance from the point in the plane $z = 0$ outside the crack to the crack's tip. Taking into account that $\sqrt{2\pi r}\sim\sqrt{\pi f}\bar{\xi}$, we rewrite these relations as

$$\frac{K_{\mathrm{I}}}{\sqrt{\pi f}} = \lim_{\xi\to 1}\bar{\xi}\sigma_z\Big|_{\eta=0};\quad \frac{K_{\mathrm{II}}}{\sqrt{\pi f}} = \lim_{\xi\to 1}\bar{\xi}\tau_{rz}\Big|_{\eta=0};\quad \frac{K_{\mathrm{III}}}{\sqrt{\pi f}} = \lim_{\xi\to 1}\bar{\xi}\tau_{z\varphi}\Big|_{\eta=0}. \tag{18}$$

An asymptotic analysis of the stress field near the crack's tip gives a series expansion of SIF. For example, K_{I} is given by

$$\sqrt{\frac{f_p}{\pi}}\frac{K^{(p)}_{\mathrm{I}}(\varphi_p)}{2\mu} = \sum_{t=0}^{\infty}{\sum_{s=-t}^{t}}' (-1)^{(t+s)/2}\left\{A^{(1)(p)}_{ts} + \frac{2}{(t+1)}A^{(2)(p)}_{t+1,\,s} + \left[\frac{4(1-\nu)}{t(2t-1)} - (1-2\nu)\right]A^{(3)(p)}_{ts}\right\} \times \exp\left(is\varphi_p\right), \tag{19}$$

where the prime over the internal sum means that it contains only the terms with even $(t + s)$. For the details of derivation, see Kushch (1998).

Table 2
$E^*_{33}(a_1, a_1/a_3)/E$ of a solid containing SO-array of penny-shaped cracks: $N = 1$

$a_1 = a_2$	a_1/a_3				
	1	2	4	8	16
5.0	0.961	0.932	0.907	0.894	0.888
4.0	0.926	0.878	0.845	0.830	0.821
3.0	0.834	0.753	0.709	0.688	0.675
2.5	0.729	0.623	0.568	0.540	0.523
2.2	0.619	0.496	0.430	0.396	0.375
2.1	0.566	0.439	0.370	0.333	0.310
2.01	0.501	0.374	0.306	0.268	0.243

Table 3
$\mu^*_{13}(a_1, a_1/a_3)/\mu$ of a solid containing SO-array of penny-shaped cracks: $N = 1$

$a_1 = a_2$	a_1/a_3				
	1	2	4	8	16
5.0	0.982	0.963	0.926	0.872	0.823
4.0	0.964	0.929	0.863	0.781	0.722
3.0	0.915	0.837	0.714	0.599	0.531
2.5	0.852	0.732	0.569	0.439	0.371
2.2	0.777	0.623	0.440	0.306	0.235
2.1	0.736	0.571	0.385	0.251	0.178
2.01	0.682	0.506	0.322	0.191	0.115

4. Numerical results

The model considered (Fig. 1) is quite general and has a number of parameters. We restrict our numerical analysis to the case of equisized cracks ($f_p = f = 1$), the solids with the following three cracks arrangement kinds will be studied:

1. the simple orthogonal (SO) array with $a_1 = a_2$, $X_p = Y_p = a_1/2$, $Z_p = (p - \frac{1}{2})a_3/N$, $p = 1$;
2. the body-centered orthogonal (BC) array with $a_1 = a_2$, $X_p = Y_p = a_1/4$ for p odd and $X_p = Y_p = 3a_1/4$ for p even, $Z_p = (p - \frac{1}{2})a_3/N$, $p = 1, 2$;
3. the quasi-random (QR) array, for which $a_1 = a_2 = a_3 = a$ and X_p, Y_p and Z_p ($p = \overline{1, N}$) are the random numbers, uniformly distributed in the interval $[0, a]$.

The values which we will calculate are the normalized Young's modulus E^*_{33}/E and shear modulus μ^*_{13}/μ given by the relations $E^*_{33} = 1/D_{3333}$ and $\mu^*_{13} = 1/4D_{1313}$, where $\hat{\mathbf{D}} = \hat{\mathbf{C}}^{-1}$ is the effective compliance tensor and $E = 2\mu(1 + \nu)$ is the Young's modulus of the cracks-free solid. To make the results for different arrays comparable, we adopt $\nu = 0.25$ for all the computations. An accuracy of the numerical data presented below can be estimated from Table 1 which shows the convergence of the effective elastic properties and the normalized opening mode SIF, $\langle K^*_{\mathrm{I}}\rangle/K_{\mathrm{I}\infty}$ with $t_{\max}$. Here, $K_{\mathrm{I}\infty}$ is the value of SIF for a single penny-shaped crack and

Table 4
$E^*_{33}(a_1, a_1/a_3)/E$ of a solid containing BC-array of penny-shaped cracks: $N = 2$

$a_1 = a_2$	a_1/a_3				
	1/2	1	2	4	8
5.0	0.961	0.922	0.862	0.812	0.787
4.0	0.925	0.852	0.752	0.688	0.656
3.0	0.830	0.680	0.496	0.404	0.361
2.5	0.723	0.517	0.283	0.170	0.125
2.2	0.611	0.387	0.162	0.066	0.041
2.1	0.559	0.336	0.127	0.044	0.024
2.01	0.500	0.280	0.094	0.026	0.011

Table 5
$\mu^*_{13}(a_1, a_3/a_1)/\mu$ of a solid containing BC-array of penny-shaped cracks: $N = 2$

$a_1 = a_2$	a_1/a_3				
	1/2	1	2	4	8
5.0	0.982	0.964	0.928	0.858	0.759
4.0	0.965	0.932	0.864	0.743	0.605
3.0	0.916	0.847	0.715	0.505	0.324
2.5	0.854	0.749	0.571	0.327	0.141
2.2	0.779	0.643	0.445	0.221	0.080
2.1	0.739	0.591	0.392	0.186	0.066
2.01	0.692	0.524	0.329	0.150	0.053

$$\langle K_{\mathrm{I}}^{*(p)} \rangle = \frac{1}{2\pi}\int_0^{2\pi} K_{\mathrm{I}}^{(p)}(\varphi_p)\,\mathrm{d}\varphi_p$$

$$= \frac{\mu}{\sqrt{\pi f_p}}\sum_{t=0}^{\infty}(-1)^t\left\{A^{(1)(p)}_{2t,\,0} + \frac{2}{(2t+1)}A^{(2)(p)}_{2t+1,\,0} + \left[\frac{2(1-\nu)}{t(4t-1)} - (1-2\nu)\right]A^{(3)(p)}_{2t,\,0}\right\}$$

is the average value of K_{I}^* on the crack's contour. The results presented in Table 1 correspond to a solid with SO-array of cracks: $N = 1$, $a_1 = a_2 = 4a_3$. We see that the convergence is rapid, especially for the effective moduli, and depends on the value $a_1 = a_2$ which determines the distance between the adjacent coplanar cracks. As calculations show, the value $t_{\max} = 7$ is sufficient in most cases to compute the effective moduli to a three-digit accuracy. The convergence rate decreases significantly only in the case of nearly touching cracks. However, even for $a_1 = 2.01$, when the closest distance between the crack's edges is as small as 1% of the crack's radius, the value $t_{\max} = 15$ provides, as a minimum, three-digit accuracy of the calculated values. Therefore, all the subsequent computations for the solids with periodic structure (SO or BC) were performed with $t_{\max} = 15$. To give some idea of computational efficiency of the method, we mention that solving the problem with above $t_{\max}$ and $N = 16$ takes about 5 min of CPU time on PC with Pentium II 266 MHz processor. However, for the solid with QR-array of cracks, the value $t_{\max} = 7$ was adopted in order to reduce the computational cost. This choice was motivated by the fact that variation of the computed values from one quasi-random structure realization to another is much greater than possible improvement in accuracy of solution by taking into account the higher harmonics.

We begin with the analysis of the effective properties of periodically cracked solids. Tables 2 and 3 give the results for E^*_{33} and μ^*_{13} of a solid weakened by the SO-array of penny-shaped cracks for

Table 6
E^*_{33}/E of a solid with SO-array of penny-shaped cracks: $N = 1$, $a_1 = a_2 = 8a_3$ (comparison with the results of previous investigators)

Reference	ε				
	0.2	0.4	0.6	0.6	1.0
Nemat-Nasser et al. (1993)	0.776	0.639	0.523	0.417	0.319
Fares (1993)	0.714	0.557	0.433	0.329	–
Eq. (17), $t_{\max} = 15$	0.763	0.614	0.486	0.386	0.260

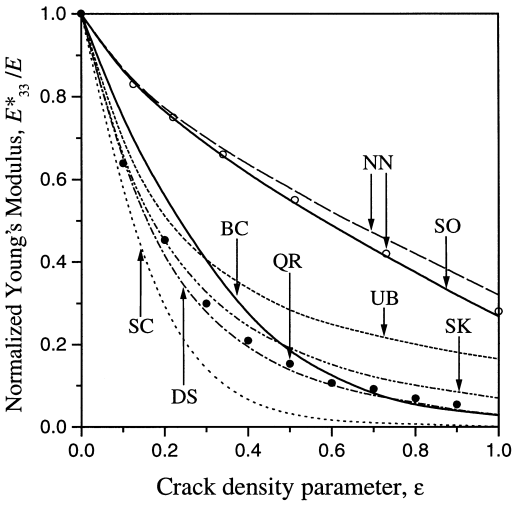

Fig. 2. Comparison of the values E^*_{33} computed by the different methods: SO — Eq. (17), SO-structure ($a_1 = a_2 = 8a_3$, $N = 1$); BC — Eq. (17), BC-structure ($a_1 = a_2 = 4a_3$, $N = 2$); QR — Eq. (17), QR-structure; SC — self-consistent scheme (Hoenig, 1979); DS — differential scheme (Laws and Dvorak, 1987); UB — upper bound (Willis, 1980); NN — Nemat-Nasser et al. (1993); SK — Sayers and Kachanov (1991).

indicated values of a_i. It is seen from these tables that the cracks reduce greatly the overall stiffness of a solid: the extent of reduction depends on the crack density parameter $\varepsilon = N/(a_1a_2a_3)$, equal to V^{-1} in our case, as well as on the lattice parameter a_1/a_3. Note that for this specific configuration, E^*_{33} remains finite even as $\varepsilon \to \infty$:

$$\lim_{a_3 \to 0} E^*_{33}/E = 1 - \pi(f/a_1)^2, \tag{20}$$

equal to the longitudinal Young's modulus of a solid with a square array of cylindrical holes.

Next, we consider a solid with the BC-array of cracks, $N = 2$. The computed values of E^*_{33} and μ^*_{13} for this solid are presented in Tables 4 and 5, respectively. Their comparison with the corresponding results presented in Tables 2 and 3 demonstrates clearly the structure effect on the effective elastic

Table 7
E^*_{33}, μ^*_{13} and $\langle K^*_I \rangle$ of solids containing QR-array of penny-shaped cracks: $N = 16$

ε	E^*_{33}/E	μ^*_{13}/μ	$\langle K^*_I \rangle / K_{I\infty}$
0.1	0.639	0.799	1.06
0.2	0.453	0.667	1.15
0.3	0.299	0.543	1.36
0.4	0.209	0.452	1.56
0.5	0.153	0.374	1.73
0.6	0.106	0.316	1.95
0.7	0.092	0.278	2.06
0.8	0.069	0.238	2.36
0.9	0.054	0.200	2.68

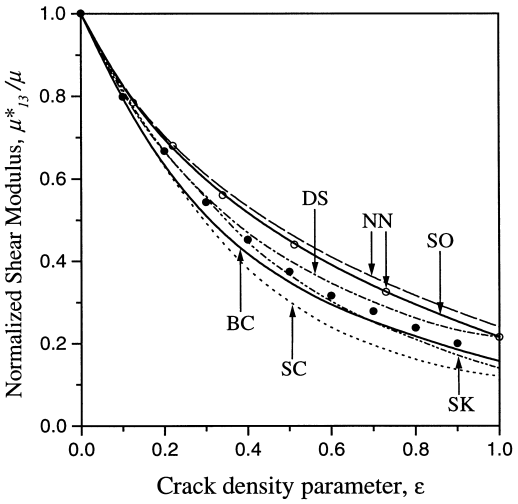

Fig. 3. Comparison of the values μ^*_{13} computed by the different methods: SO — Eq. (17), SO-structure ($a_1 = a_2 = 8a_3$, $N = 1$); BC — Eq. (17), BC-structure ($a_1 = a_2 = 4a_3$, $N = 2$); QR — Eq. (17), QR-structure; SC — self-consistent scheme (Hoenig, 1979); DS — differential scheme (Laws and Dvorak, 1987); NN — Nemat-Nasser et al. (1993); SK — Sayers and Kachanov (1991).

moduli: the BC-array of cracks induces much greater stiffness decrease than the SO-array with the same crack density value; in particular, for BC-structure, $E^*_{33} \to 0$ as $\varepsilon \to \infty$.

The effective stiffness of a solid containing SO-arrays of equal penny-shaped cracks was determined by Nemat-Nasser et al. (1993), who used a Fourier series technique, and by Fares (1993), who used the boundary element method. The results of these investigators for E^*_{33} for indicated values of ε with $a_1 = a_2 = 8a_3$ are compared with the results obtained by the present investigation in Table 6. It may be noted that the solution obtained by Nemat-Nasser et al. (1993), who used an assumption of uniform homogenization eigenstrains, exactly corresponds to our solution with $t_{\max} = 1$ in Eq. (15). Comparison of these data with the accurate values obtained from Eq. (17) with $t_{\max} = 15$ shows that the Nemat-Nasser's technique gives a reasonably good approximation at moderate crack densities ($\varepsilon < 0.5$ for the chosen configuration). For greater values of damage parameter, the effect of higher harmonics must be taken into account. Note also, that an alternate variant of the above mentioned technique, based on the piece wise constant approximation of the homogenization eigenstrains, gives much better agreement with

Table 8
$\langle K^*_1 \rangle / K_{I\infty}$ in a solid with SO-array of penny-shaped cracks: $N = 1$

a_1/a_2	a_1/a_3				
	1	2	4	8	16
5.0	1.01	0.93	0.74	0.54	0.40
4.0	1.03	0.92	0.72	0.53	0.39
3.0	1.08	0.96	0.75	0.56	0.42
2.5	1.19	1.08	0.87	0.66	0.49
2.2	1.39	1.28	1.08	0.86	0.64
2.1	1.55	1.45	1.23	1.00	0.75
2.01	2.02	1.87	1.56	1.24	0.93

Table 9
$\langle K_I^* \rangle / K_{I\infty}$ in a solid with BC-array of penny-shaped cracks: $N = 2$

a_1/a_2	a_1/a_3				
	1/2	1	2	4	8
5.0	1.02	1.06	1.02	0.83	0.62
4.0	1.04	1.11	1.10	0.89	0.68
3.0	1.10	1.24	1.45	1.35	1.12
2.5	1.21	1.38	1.86	2.07	1.71
2.2	1.41	1.58	2.24	2.90	2.42
2.1	1.58	1.76	2.51	3.47	3.44
2.01	2.04	2.28	3.41	5.32	6.52

the accurate solution (the hollow circles in Fig. 2). Unlike the Nemat-Nasser's approach, where an interaction of *all* the cracks is accounted for (although only in approximate way), in the work by Fares (1993), the numerical BEM technique was applied only to a *finite* number of interacting cracks. As a result, the numerical data reported there, greatly underestimate the exact solution.

However, in a majority of works on elasticity of cracked solids, a somewhat different geometrical model pioneered by Hoenig (1979) is adopted. Namely, the equally sized and oriented penny-shaped cracks are supposed to be randomly, statistically uniformly distributed in an isotropic medium. It is obvious that the model considered by us allows to approach this structure type. To this end, we consider the cubic unit cell ($a_1 = a_2 = a_3$) and determine the position of the crack centers $\mathbf{R}_p$ with the aid of random number generator. To make the results independent of the specific configuration chosen, the computed data were averaged over 30 numerical experiments of the same kind. As calculations show, the number of cracks $N = 16$ is reasonably large to make the results only slightly sensitive to N as well as to the shape of the averaging volume (structure cell). The computed values of E_{33}^*, μ_{13}^* and $\langle K_I^* \rangle / K_{I\infty}$ for solids containing QR-array of cracks are summarized in Table 7 and presented by the

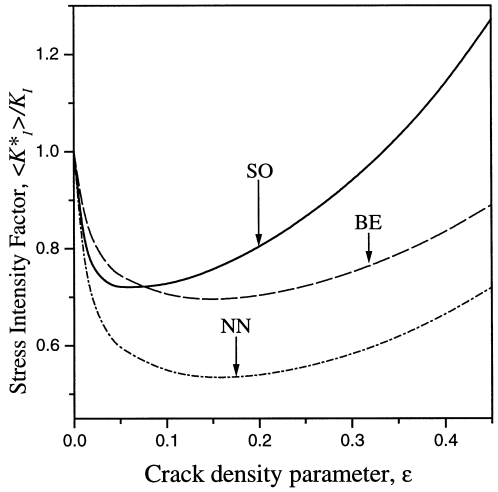

Fig. 4. Comparison of the values $\langle K_I^* \rangle$ computed by the different methods: SO — Eq. (17), SO-structure ($a_1 = a_2 = 4a_3$, $N = 1$); NN — Nemat-Nasser et al. (1993) (uniform eigenstrains); BE — boundary element method (Fares, 1993).

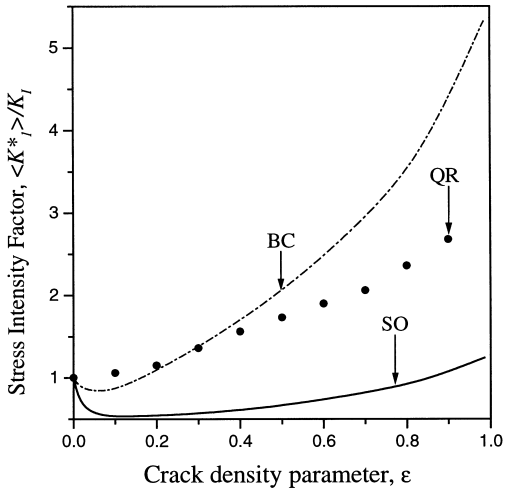

Fig. 5. Effect of structure type on $\langle K_I^* \rangle$: SO — Eq. (17), SO-structure ($a_1 = a_2 = 8a_3$, $N = 1$); BC — Eq. (17), BC-structure ($a_1 = a_2 = 4a_3$, $N = 2$); QR — Eq. (17), QR-structure.

solid circles in Figs. 2, 3 and 5. It is of interest to compare these data with those obtained by other authors. Some results of such a comparison are presented in Figs. 2 and 3. Interestingly, the values E_{33}^* calculated by us for a QR-structure (solid circles) meet the upper variational bound by Willis (1980) and lie on the tiny interval between the values predicted by Sayers and Kachanov (1991) and by the differential method (e.g., Laws and Dvorak, 1987). The self-consistent scheme (Hoenig, 1979) underestimates these results. Note that the values of E_{33}^* for a solid with SO-array of cracks ($a_1 = a_2 = 8a_3$, $N = 1$) reported by Nemat-Nasser et al. (1993) as well as those obtained from Eq. (17) lie far above the Willis' bound. On the contrary, the Young's modulus of a solid with BC-array of cracks ($a_1 = a_2 = 4a_3$, $N = 2$) for $\varepsilon > 0.3$ meets the variational bound and, for $\varepsilon > 0.4$, is close enough to the data obtained for the solid with randomly placed cracks. Hence, this simple periodic structure may serve as some approximation of a randomly cracked body.

The analogous comparison for the μ_{13}^*/μ are presented in Fig. 3. The values of effective shear modulus obtained from the theories compared lie more closely than in the previous case. Also, the accurate values μ_{13}^* for SO-, BC- and QR-structures are not so far from one another meaning that the effective shear modulus is relatively less structure-sensitive parameter. Once again, we note that the values of μ_{13}^* for the BC- and QR-structures are close to each other. Thus, the BC-structure is a better approximation of randomly cracked body than a medium with SO-array of cracks.

A limited number of works are known in literature where the SIF in a cracked solid is studied. The reason is, above all, that SIF is essentially local and highly structure-sensitive parameter. Its reliable prediction requires the structure of a cracked solid to be specified in detail and the corresponding boundary-value problem to be solved with sufficient accuracy. The method presented here provides calculation of a detailed SIF distribution along the perimeter of each specific crack (Eq. (19)) as well as its mean value (Eq. (20)). In Tables 8 and 9, the values $\langle K_I^* \rangle / K_{I\infty}$ are presented for the solids with SO- and BC-arrays of cracks, respectively. It is seen from these tables that the cracks interact in complex ways. For the SO-structure, the overlapping cracks shield each other and decrease the SIF, whereas the adjacent coplanar cracks amplify each other and, thus, increase it. The resulting value appears to be

strongly dependent on the ratio of periods a_1, a_2 and a_3. The same tendency takes place for the BC-structure; however, in this case, $\langle K_I^* \rangle$ does not reduce with a_1/a_3 but grows rapidly, especially for the closely packed cracks in the Oxy-plane.

Now, we compare our results with those reported by Nemat-Nasser et al. (1993) and Fares (1993) using the fact that SIF is proportional to the crack opening displacement (e.g., Irwin, 1962). The dependencies $\langle K_I^* \rangle(\varepsilon)$ for a solid with SO-array of cracks ($a_1 = a_2 = 4a_3,\ N = 1$) obtained by these methods are plotted in Fig. 4. It should be noted that all the theories predict correctly the non-monotonic behavior of $\langle K_I^* \rangle$; at the same time, satisfactory agreement of absolute values takes place only for a very small crack density. This is quite natural because to provide the convergence of the series (20), the higher harmonics should be taken into account (see Table 1). Finally, the values $\langle K_I^* \rangle(\varepsilon)$ for the solids containing SO-array ($a_1 = a_2 = 8a_3, N = 1$), BC-array ($a_1 = a_2 = 4a_3, N = 2$) and QR-array ($N = 16$) are presented in Fig. 5. In the last case, K_I^* was averaged over all the cracks within the unit cell and over 30 structure realizations. These data, above all, again demonstrate clearly the structural sensitivity of this parameter.

5. Concluding remarks

The method presented here is accurate and efficient from the computational standpoint. To our knowledge, this is the first time when a complete solution is obtained for the elasticity problem containing periodically distributed penny-shaped cracks. The model considered is general enough and provides modeling of both the periodically and randomly cracked solids. As calculations show, the mechanical properties of a cracked body appears to be structure-sensitive parameter: this suggests that the structure parameters should be taken into account to a maximum possible extent. To this end, a certain experimental data or physical assumptions relating the structure parameters are required to choose the geometrical model, approaching the microstructure of actual material and, thus, to provide a reliable prediction of its effective stiffness and strength.

Acknowledgements

This work was made possible in part by Award #UE1-334 of the US Civilian Research and Development Foundation for the Independent States of the Former Soviet Union (CRDF). The authors also acknowledge the Cornell Theory Center for the supercomputing support. A.S. Sangani also acknowledges the support from the National Science Foundation under grant CTS-9632227.

Appendix A. Partial vectorial solutions of the Lame equation in spheroidal coordinates

The following partial vectorial solutions of Eq. (2) have been derived by Kushch (1996): constrained at $\|\mathbf{r}\| \to \infty$, or singular $\mathbf{S}_{ts}^{(i)} = \mathbf{S}_{ts}^{(i)}(\mathbf{r}, f)$:

$$\mathbf{S}_{ts}^{(1)} = \mathbf{e}_1 F_{t+1}^{s-1} - \mathbf{e}_2 F_{t+1}^{s+1} + \mathbf{e}_3 F_{t+1}^{s};\ \mathbf{S}_{ts}^{(2)} = \frac{1}{t}\left[\mathbf{e}_1(t+s)F_t^{s-1} + \mathbf{e}_2(t-s)F_t^{s+1} + \mathbf{e}_3 s F_t^{s}\right];$$

$$\begin{aligned}\mathbf{S}_{ts}^{(3)} = \mathbf{e}_1\Big\{ &-(x-iy)D_2F_{t-1}^{s-1} - \left[\left(\xi^{(0)}\right)^2 - 1\right]D_1F_t^s + (t+s-1)(t+s)\beta_{-(t+1)}F_{t-1}^{s-1}\Big\} + \mathbf{e}_2\Big\{(x\\ &+iy)D_1F_{t-1}^{s+1} - \left[\left(\xi^{(0)}\right)^2 - 1\right]D_2F_t^s - (t-s-1)(t-s)\beta_{-(t+1)}F_{t-1}^{s+1}\Big\} + \mathbf{e}_3\Big[zD_3F_{t-1}^{s}\\ &-\left(\xi^{(0)}\right)^2 D_3F_t^s + (t+s)(t-s)\beta_{-(t+1)}F_{t-1}^{s}\Big];\end{aligned} \tag{A1}$$

constrained at $\|\mathbf{r}\|\to 0$, or regular $\mathbf{s}_{ts}^{(i)} = \mathbf{s}_{ts}^{(i)}(\mathbf{r}, f)$:

$$\mathbf{s}_{ts}^{(1)} = \mathbf{e}_1 f_{t-1}^{s-1} - \mathbf{e}_2 f_{t-1}^{s+1} + \mathbf{e}_3 f_{t-1}^{s};\ \mathbf{s}_{ts}^{(2)} = \frac{1}{t+1}\left[\mathbf{e}_1(t-s+1)f_t^{s-1} + \mathbf{e}_2(t+s+1)f_t^{s+1} - \mathbf{e}_3 s f_t^{s}\right];$$

$$\begin{aligned}\mathbf{s}_{ts}^{(3)} = \mathbf{e}_1\Big\{ &-(x-iy)D_2f_{t+1}^{s-1} - \left[\left(\xi^{(0)}\right)^2 - 1\right]D_1f_t^s + (t-s+1)(t-s+2)\beta_t f_{t+1}^{s-1}\Big\} + \mathbf{e}_2\Big\{(x\\ &+iy)D_1f_{t+1}^{s+1} - \left[\left(\xi^{(0)}\right)^2 - 1\right]D_2f_t^s - (t+s+1)(t+s+2)\beta_t f_{t+1}^{s+1}\Big\} + \mathbf{e}_3\Big[zD_3f_{t+1}^{s}\\ &-\left(\xi^{(0)}\right)^2 D_3f_t^s - (t+s+1)(t-s+1)\beta_t F_{t+1}^{s}\Big];\end{aligned} \tag{A2}$$

where

$$\beta_t = \frac{t+5-\nu}{(t+1)(2t+3)};\quad t = 1, 2, \ldots; |s| \le t.$$

In Eqs. (A1) and (A2), the following notations are used:

$$\mathbf{e}_1 = \left(\mathbf{e}_x + i\mathbf{e}_y\right)/2,\quad \mathbf{e}_2 = \bar{\mathbf{e}}_1 = \left(\mathbf{e}_x - i\mathbf{e}_y\right)/2,\quad \mathbf{e}_3 = \mathbf{e}_z;$$

$$D_1 = (\partial/\partial x - i\partial/\partial y),\quad D_2 = \bar{D}_1 = (\partial/\partial x + i\partial/\partial y),\quad D_3 = \partial/\partial z. \tag{A3}$$

The functions $F_t^s = F_t^s(\mathbf{r}, f)$ and $f_t^s = f_t^s(\mathbf{r}, f)$ are the singular and regular, respectively, solid spheroidal harmonics, appropriate form of whose in oblate case is

$$F_t^s(\mathbf{r}, f) = i^{t+1}Q_t^{-s}\left(i\bar{\xi}\right)Y_t^s(\eta, \varphi),\quad f_t^s(\mathbf{r}, f) = i^{-t}P_t^{-s}\left(i\bar{\xi}\right)Y_t^s(\eta, \varphi),$$

where $Y_t^s(\eta, \varphi) = P_t^s(\eta)\exp(is\varphi)$ are the scalar surface harmonics and P_t^s and Q_t^s are the associated Legendre polynomials of first and second kind, respectively.

References

Benveniste, Y., 1986. On the Mori–Tanaka's method in cracked bodies. Mech. Res. Comm 13, 193–201.
Budiansky, B., O'Connell, 1976. Elastic moduli of a cracked solid. Int. J. Solids Structures 12 81–97.
Fares, N., 1993. Effective stiffness of a periodically cracked 3D solid. Int. J. Fracture 62, 149–162.
Golovchan, V.T., Guz, A.N., Kohanenko, Yu., Kushch, V.I., 1993. Mechanics of Composites. Statics of Materials, vol. 1. Naukova dumka, Kiev (In Russian).
Hashin, Z., 1988. The differential scheme and its application to cracked materials. J. Mech. Phys. Solids 36, 719–734.
Heyney, F.S., Pomphrey, N., 1982. Self consistent elastic moduli of a cracked solid. Geohpys. Res. Lett 9, 903–906.

Hobson, E.W., 1931. The Theory of Spherical and Ellipsoidal Harmonics. Cambridge University Press, MA.
Hoenig, A., 1979. Elastic moduli of a non-randomly cracked body. Int. J. Solids Structures 15, 137–154.
Irwin, G.R., 1962. Crack-extension force for a part-through crack in a plate. J. Appl. Mech 29, 651–654.
Kachanov, M., 1987. Elastic solids with many cracks: a simple method of analysis. Int. J. Solids Structures 23, 23–43.
Kachanov, M., 1993. Elastic solids with many cracks and related problems. In: Hutchinson, J.W., Wu, T.Y. (Eds.), Advances in Applied Mechanics, vol. 30. Academic Press, New York, pp. 259–445.
Kushch, V.I., 1996. Elastic equilibrium of a medium containing finite number of aligned spheroidal inclusions. Int. J. Solids Structures 33, 1175–1189.
Kushch, V.I., 1998. Interacting cracks and inclusions in a solid by the multipole expansion method. Int. J. Solids Structures 35, 1187–1198.
Kushch, V.I., 1997. Microstresses and effective elastic moduli of a solid reinforced by periodically distributed spheroidal inclusions. Int. J. Solids Structures 34, 1353–1366.
Laws, N., Brockenbrough, J.R., 1987. The effect of microcrack systems on the loss of stiffness of brittle solids. Int. J. Solids Structures 23, 1247–1268.
Laws, N., Dvorak, G.J., 1987. The effect of fibre breaks and aligned penny-shaped cracks on the stiffness and energy release rates in unidirectional composites. Int. J. Solids Structures 23, 1269–1283.
Nemat-Nasser, S., Yu, N., Hori, M., 1993. Solids with periodically distributed cracks. Int. J. Solids Structures 30, 2071–2095.
Sangani, A.S., Mo, G., 1997. Elastic interactions in particulate composites with perfect as well as imperfect interfaces. J. Mech. Phys. Solids 45, 2001–2031.
Salganik, R.L., 1973. Mechanics of bodies with many cracks. Izv. AN SSSR Mechanika tverdogo tela 8, 149–158. (English translation Mech. Solids 8, 135–143).
Sayers, C.M., Kachanov, M., 1991. A simple technique for finding effective elastic constants of cracked solids for arbitrary orientation statistics. Int. J. Solids Structures 27, 621–680.
Willis, J.R., 1980. A polarization approach to the scattering of elastic waves. Part II: Multiple scattering from inclusions. J. Mech. Phys. Solids 28, 307–327.